Available online at www.sciencedirect.com
ScienceDirect
Mechatronics 18 (2008) 141–152
MECHATRONICS

Modeling and control of shape memory alloy actuators using Preisach model, genetic algorithm and fuzzy logic

Kyoung Kwan Ahn *, Nguyen Bao Kha

Graduate School of Mechanical and Automotive Engineering, University of Ulsan, San 29, Muger 2dong, Nam-gu, Ulsan 680-764, Republic of Korea

Received 4 January 2006; accepted 23 October 2007

Abstract

Shape memory alloy (SMA) actuators, which have the ability to return to a predetermined shape when heated, have many potential applications in aeronautics, surgical tools, robotics and so on. Nonlinearity hysteresis effects existing in SMA actuators present a problem in the motion control of these smart actuators. This paper investigates the control problem of SMA actuators in both simulation and experiment. In the simulation, the numerical Preisach model with geometrical interpretation is used for hysteresis modeling of SMA actuators. This model is then incorporated in a closed loop PID control strategy. The optimal values of PID parameters are determined by using genetic algorithm to minimize the mean squared error between desired output displacement and simulated output. However, the control performance is not good compared with the simulation results when these parameters are applied to the real SMA control since the system is disturbed by unknown factors and changes in the surrounding environment of the system. A further automated readjustment of the PID parameters using fuzzy logic is proposed for compensating the limitation. To demonstrate the effectiveness of the proposed controller, real time control experiment results are presented.

Keywords: Fuzzy; Genetic algorithm; Hysteresis; PID; Preisach model; Self tuning; SMA actuator

1. Introduction

The last decade has seen a growing interest in the field of decreasing in size and weight of the control and robotic systems, so must their respective components. Actuators, the driving mechanism behind these systems, play an important role in the system design and typically rely on electric, hydraulic, and pneumatic technology. Unfortunately, there is a drastic reduction in the power that these forms of actuations can deliver as they are scaled down in size and weight. This restriction has opened investigation of several novel smart actuators such as electromagnetics, piezoelectrics, and shape memory alloys.

Among these technologies, the shape memory alloy (SMA) actuators, which have the ability to generate significant strains (up to 8%) in response to a temperature change, have the clear advantage in strength to weight ratio. With the high inherent strength of the SMA actuators comes the advantage of being able to implement direct drive devices. Direct drive devices eliminate the use of gears with their inherent problems of backlash and wear. Their ability to generate large strains has promoted their use as an ''artificial muscle''. The high force/mass ratio, silent and smooth motions of these actuators has been applied in numerous applications [1,2].

The ability to ''memorize'' a specific shape is a result of physical changes in the SMA actuators. This occurs through a solid-state phase change by molecular rearrangement. The two phases that occur in the SMA, are martensite and austenite. At higher temperatures, the material is in the austenite phase. As the temperature is lowered, the material changes to the martensite phase and grows until sufficiently low temperatures. These changes occur in a highly nonlinear fashion, introducing the significant hysteresis in the actuator response. Hysteresis behavior introduces delays

* Corresponding author. Tel.: +82 52 259 2282; fax: +82 52 259 1680.
E-mail address: kkahn@ulsan.ac.kr (K.K. Ahn).

0957-4158/$ - see front matter © 2007 Published by Elsevier Ltd.
doi:10.1016/j.mechatronics.2007.10.008

and leads to inaccuracy in the motion control of SMA actuators.

The hysteresis in SMA actuators is a complex nonlinearity with memory that may result in multiple outputs for a given input, depending on its time history. To obtain high control performance, it is necessary to develop the hysteresis models that not only capture all of the essential characteristics relevant to the hysteresis of the SMA actuators, but also are suitable for control system design and real time implementation. Development of this type of model, its experimental verification and control application are addressed in this paper.

The hysteresis model in ferroelectric, electromagnetics, magnetostrictive, piezoceramics and SMA actuators has been addressed in several reports [3–9]. Two distinct types of model have been proposed to capture the hysteretic characteristics. The first type of models were derived from the physics of hysteresis and combined with empirical factors to describe the models [3,11–13]. However, these models are not easily used in control systems, as the physical basis of some of the hysteresis characteristics is not completely understood. This requires considerable effort in identifying and tuning the model parameters in order to describe the hysteresis phenomenon accurately. The second type of model is based on the phenomenological nature and describes the phenomena mathematically. Among these, the Preisach model is a well known approach to model the hysteresis functions [4–10]. Although the Preisach model does not provide physical insight into the problem, it provides a means of developing phenomenological model that is capable of producing behaviors similar to those of the physical systems. Therefore, it is a convenient tool for simulation and control applications. In this paper, the numerical Preisach model based on geometrical interpretation is used for the hysteresis modeling. This model is then incorporated in a closed loop PID control in simulation environment. The values of PID parameters are determined by using genetic algorithm to minimize the mean squared error between desired output displacement and simulated output.

However, the PID controller with parameters obtained from simulation is not good when it is applied to the real SMA control since the system is disturbed by unknown factors and changes in the surrounding environment. Therefore, a further readjustment of the PID parameters using fuzzy logic is proposed to enhance the control and adaptation ability with respect to the external variations. The optimal parameters obtained from the simulation are used as the initial values of the PID controller. The proposed controller tunes the PID parameters from these initial values by integrating the fuzzy inference and producing a fuzzy adaptive PID controller. Experimental results show that the proposed algorithm can be used to improve the accuracy of the motion control and reduce the hysteresis nonlinearity effect of SMA actuators.

The remainder of the paper is organized as follows. Section 2 reviews the introduction to the Preisach model and its geometrical interpretation. The numerical Preisach model and the identification results are also presented in this section. In Section 3, the Preisach model is incorporated in the PID closed loop control scheme to investigate the possibility of PID algorithm in the SMA control. The application of genetic algorithm to find the optimal parameters of PID controller is shown in this section. Next, the design of self tuning fuzzy PID controller along with the experiment results of the SMA position control are decribed in Section 4. Concluding remarks are provided in Section 5.

2. Hysteresis modeling of SMA actuator using Preisach model

2.1. Preisach model

The main assumption made in the Preisach model is that the system consists of a parallel summation of a continuum of weighted hysteresis operators $\gamma_{\alpha\beta}$. Each of these operators is represented by a rectangular loop on the input–output diagram shown in Fig. 1. The numbers α and β correspond to "up" and "down" switching values of input, respectively.

As the input varies with time, each relay adjusts its output according to the current input value and the weighted sum of these outputs provides the system output. Along with the set of operators $\gamma_{\alpha\beta}$, there is an arbitrary weight function $\mu(\alpha,\beta)$, which is termed the Preisach function. Then the Preisach model is written as follows:

$$y(t) = \iint_{\alpha\geqslant\beta} \mu(\alpha,\beta)\gamma_{\alpha\beta}[u(t)]\mathrm{d}\alpha\mathrm{d}\beta \tag{1}$$

The collection of weights $\mu(\alpha,\beta)$ describes the relative contribution of each relay in the overall hysteresis. According to this model, the same input $u(t)$ is applied to all of the hysteresis operators. Their outputs are multiplied by $\mu(\alpha,\beta)$ and integrated over all appropriate values of α and β and the system output is then obtained.

2.2. Geometrical interpretation of Preisach model

It is assumed that there is a one-to-one correspondence between the operator $\gamma_{\alpha\beta}$ and the point (α,β) on the half plane $\alpha \geqslant \beta$. This is called the Preisach plane. In other words, each point in the Preisach plane can be identified with only one particular hysteresis operator whose switching values are equal to the α and β coordinates of the point. The function $\mu(\alpha,\beta)$ is assumed to be zero outside the triangle **T** in Fig. 2. The hypotenuse of this triangle is the line $\alpha = \beta$, with the coordinates of the vertex, representing the maximal value of the input that is being modeled.

To start the discussion, consider the case of hysteresis formation in SMA actuator when the driving input $u(t)$ is current, and the resulting output is displacement $y(t)$. When the current to the SMA actuator is zero, the output of all of the operators is zero.

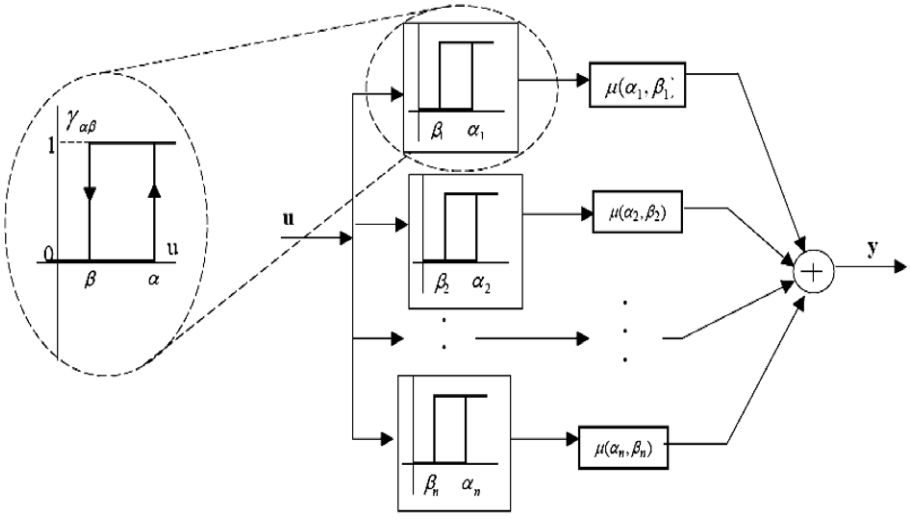

Fig. 1. Preisach model schematic.

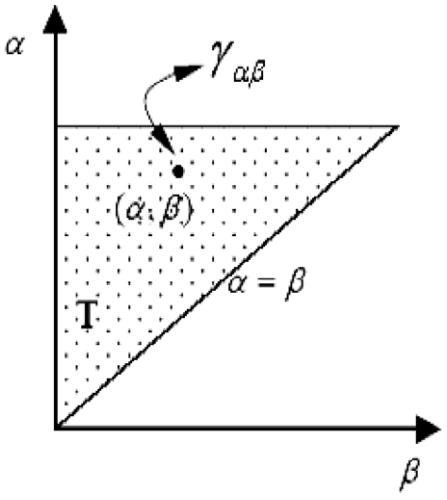

Fig. 2. Preisach plane.

It is assumed that the input is monotonically increasing to a value α_1, as shown in Fig. 3, and the outputs of all of the hysteresis operators with an α switching value less than α_1 become equal to $+1$. Geometrically, this leads to the subdivision of the triangle **T** into two sets: $S^+(t)$ consisting of point (α,β), where the output is $+1$, and $S^0(t)$, where the output is zero. This subdivision is made by the line $\alpha = u(t)$ that moves upwards as the input is increased. This upward motion is terminated when the input reaches the maximum value of α_1.

Next, the input is monotonically decreased from $\alpha_1$to a value β_1. As the input is decreased, the outputs of all of the hysteresis operators in the set $S^+(t)$ with β switching values greater than β_1 become equal to zero. This changes the previous subdivision of **T** into two sets again. The interface between $S^+(t)$ and $S^0(t)$ has two links at this point including both horizontal and vertical. As illustrated in Fig. 4, the vertical link moves from right to left as the current is monotonically decreased from α_1 to β_1. The vertical

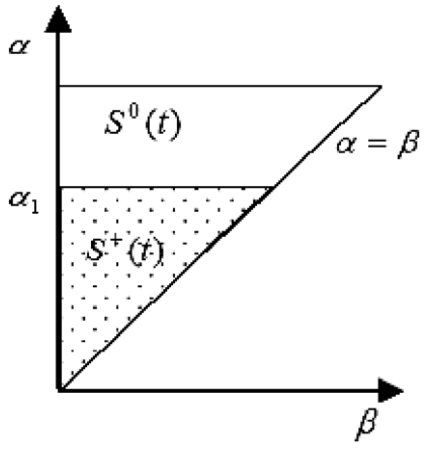

Fig. 3. Division of the triangle due to a increasing input α_1.

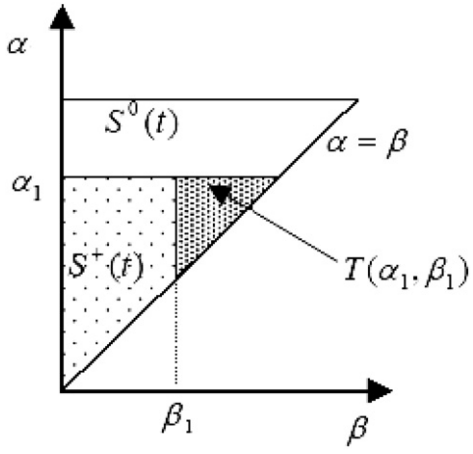

Fig. 4. Division of the triangle due to a decreasing input β_1.

line is $\beta = u(t)$. The motion of the vertical link is terminated when the input reaches a minimum value of β_1.

By generating this analysis with the case of increasing or decreasing input, the following conclusion is reached. At any instant of time, the triangle **T** is subdivided into two sets: $S^+(t)$ and $S^0(t)$ corresponding to the output of the hysteresis operators is +1 or zero. The interface between $S^+(t)$ and $S^0(t)$ is the staircase line whose vertices have α and β coordinates, respectively with local maxima and minima of the input at a previous instant of time.

Thus, at any instant of time the integral in (1) can be expressed by

$$y(t) = \iint_{S^+(t)} \mu(\alpha,\beta)\gamma_{\alpha\beta}[u(t)]\mathrm{d}\alpha\mathrm{d}\beta - \iint_{S^0(t)} \mu(\alpha,\beta)\gamma_{\alpha\beta}[u(t)]\mathrm{d}\alpha\mathrm{d}\beta \tag{2}$$

where $\gamma_{\alpha\beta}u(t) = 0$, $\forall(\alpha,\beta) \in S^0(t)$ and $\gamma_{\alpha\beta}u(t) = 1$, $\forall(\alpha,\beta) \in S^+(t)$, then this expression becomes

$$y(t) = \iint_{S^+(t)} \mu(\alpha,\beta)\mathrm{d}\alpha\mathrm{d}\beta \tag{3}$$

From this expression, the output of the Preisach model depends on the subdivision of triangle **T**. This subdivision is determined by an interface which depends on the past extremum values of the input.

2.3. Numerical Preisach model

To apply the classical Preisach hysteresis model to SMA actuators, many difficulties are encountered. It requires the evaluation of double integrals in (1) or (3). This is a time consuming procedure that makes the use of the Preisach model difficult in practical applications. Furthermore, the other problems are to determine the number of required hysteresis operators $\gamma_{\alpha\beta}$ and their associated Preisach functions $\mu(\alpha,\beta)$. An identification procedure and a discrete numerical implementation were developed [10], which are rederived for the case of displacement versus current hysteresis as follows.

The basic idea is to identify the function $F(\alpha,\beta)$ that is defined as follows:

$$F(\alpha_1,\beta_1) = y_{\alpha_1} - y_{\alpha_1\beta_1} \tag{4}$$

where y_{α_1} is the output at the current value of α_1, and $y_{\alpha_1\beta_1}$ is the output after the current has been decreased to β_1 from its maximum value of α_1. This function is equal to the output increments along the first order transition curves. These curves are defined as follows: the input current is monotonically increased from zero to some value α_1 and then decreased to a value β_1 that is greater than zero. The term "first order" is used to emphasize the fact that each of these curves is formed after the first reversal of the input.

From Fig. 4, the fact that the integral over the area $T(\alpha_1,\beta_1)$ is equal to the difference in the hysteresis outputs of current values of α_1 and β_1 is found

$$\iint_{T(\alpha_1,\beta_1)} \mu(\alpha,\beta)\mathrm{d}\alpha\mathrm{d}\beta = F(\alpha_1,\beta_1) \tag{5}$$

The set$S^+(t)$can be subdivided into $n(t)$ trapezoids Q_k. As a result, it can be expressed as:

$$\iint_{S^+(t)} \mu(\alpha,\beta)\mathrm{d}\alpha d\beta = \sum_{k=1}^{n(t)} \iint_{Q_k(t)} \mu(\alpha,\beta)\mathrm{d}\alpha\mathrm{d}\beta \tag{6}$$

where n trapezoids Q_k may change with time.

Each trapezoid Q_k can be represented as a difference of two triangles $T(M_k,m_{k-1})$ and $T(M_k,m_k)$, where M_k and m_k denote the maximum and minimum points of the input history. Therefore,

$$\iint_{Q_k(t)} \mu(\alpha,\beta)\mathrm{d}\alpha\mathrm{d}\beta = \iint_{T(M_k,m_{k-1})} \mu(\alpha,\beta)\mathrm{d}\alpha\mathrm{d}\beta - \iint_{T(M_k,m_k)} \mu(\alpha,\beta)\mathrm{d}\alpha\mathrm{d}\beta \tag{7}$$

Through (5), it is known that

$$\iint_{T(M_k,m_{k-1})} \mu(\alpha,\beta)\mathrm{d}\alpha\mathrm{d}\beta = F(M_k,m_{k-1}), \tag{8}$$

and

$$\iint_{T(M_k,m_k)} \mu(\alpha,\beta)\mathrm{d}\alpha\mathrm{d}\beta = F(M_k,m_k) \tag{9}$$

Thus, (7) can be rewritten as follows:

$$\iint_{Q_k(t)} \mu(\alpha,\beta)\mathrm{d}\alpha\mathrm{d}\beta = F(M_k,m_{k-1}) - F(M_k,m_k) \tag{10}$$

From (3), (6) and (10), the output $y(t)$ of the hysteresis nonlinearity is written as follows:

$$y(t) = \sum_{k=1}^{n(t)} [F(M_k,m_{k-1}) - F(M_k,m_k)] \tag{11}$$

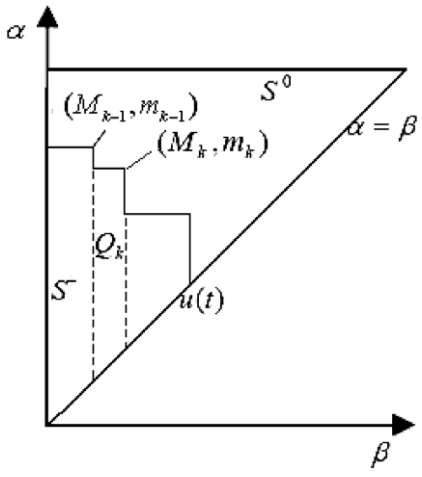

Fig. 5. Triangle **T** for numerical implementation of the Preisach model corresponding to a decreasing input current signal.

In the case that the input is monotonically decreasing, as shown in Fig. 5, the final link of the interface is a vertical one, thus: $m_n = u(t)$. Consequently, Eq. (11) can be written as

$$y(t) = \sum_{k=1}^{n(t)-1} [F(M_k, m_{k-1}) - F(M_k, m_k)] + [F(M_n, m_{n-1}) - F(M_n, u(t))] \quad (12)$$

or

$$y(t) = \sum_{k=1}^{n(t)-1} [y_{M_k,m_k} - y_{M_k,m_{k-1}}] + [y_{M_n,u(t)} - y_{M_n,m_{n-1}}] \quad (13)$$

If the input is monotonically increasing, as shown in Fig. 6, the final link of the interface is a horizontal one, $m_n = M_n(t) = u(t)$, and Eq. (11) becomes:

$$y(t) = \sum_{k=1}^{n(t)-1} [F(M_k, m_{k-1}) - F(M_k, m_k)] + F[u(t), m_{n-1}] \quad (14)$$

or

$$y(t) = \sum_{k=1}^{n(t)-1} [y_{M_k,m_k} - y_{M_k,m_{k-1}}] + [y_{u(t)} - y_{u(t),m_{n-1}}] \quad (15)$$

Using the above expressions, the output of the Preisach model can be calculated from an input, a set of first order transition curves, and an input history that is specified by the user.

To implement this algorithm, there are two main steps for hysteresis modeling. First, a square mesh covering the triangle **T** is created. The number of switching points in the Preisach plane, as shown in Fig. 2, can be selected by the user. During this stage, a discrete set of first order transition curves is entered. With each value of the switching point (α, β) in the Preisach plane, the input current is monotonically increased to α and then decreased to β. At the vertex of each first order transition curve, the values of the output displacement $(y_{\alpha_1}, y_{\alpha_1\beta_1})$ are measured. The value of the function $F(\alpha, \beta)$ is obtained from Eq. (4). Then, a mesh of values for the function $F(\alpha, \beta)$ are determined from the experimental data.

At the second stage, an input history and the current values of the input are entered. Using these data, the alternating series of dominant input extrema (M_k, m_k) and (M_k, m_{k-1}) must be determined from the input current to SMA actuators and updated at each instant of time. All terms in the formulas (12) and (14) are computed from these values: M_k, m_k, m_{k-1} and the mesh value $F(\alpha, \beta)$. This is done first of all by determining the particular square (or triangle) cells to which points (M_k, m_k), (M_k, m_{k-1}), and $(M_n, u(t))$ belong, and then by computing the value of $F(\alpha, \beta)$at these points by means of interpolation of the mesh values of $F(\alpha, \beta)$ at the vertices of these cells. Finally, the output is calculated using the Preisach model parameters $F(\alpha, \beta)$, in (12) (or (14)) for the case of decreasing (or increasing) of the input. The output of the hysteresis nonlinearity can also be computed by using Eqs. (13) and (15) with a similar procedure.

2.4. Identification results

Fig. 7 shows the experimental apparatus for the SMA positioning system. In the experimental setup for hysteresis modeling and control, a small tensile SMA wire (made by Memory–Metalle GmbH) is used with these specifications: heat current: ca. 2 V/0.85 A, gen. force: 8 N, and displacement: ca.5 mm. This SMA wire has a one-way shape memory effect. The displacement was measured by a high precision potentiometer and fed to the computer through an A/D Advantech PCI – 1711 card. The control current that was applied to the SMA wire obtained from a D/A card and a V/I converter. This system is controlled in real-time by using Advantech PCI-1711 Card with Real-time Windows Target Toolbox of Matlab.

The switching points used in this program are shown in Fig. 8. It should be known that if more switching points are

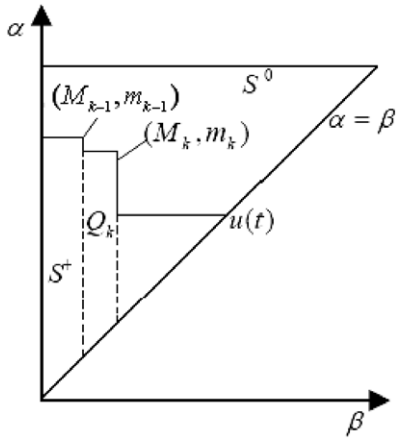

Fig. 6. Triangle **T** for numerical implementation of the Preisach model corresponding to an increasing input current signal.

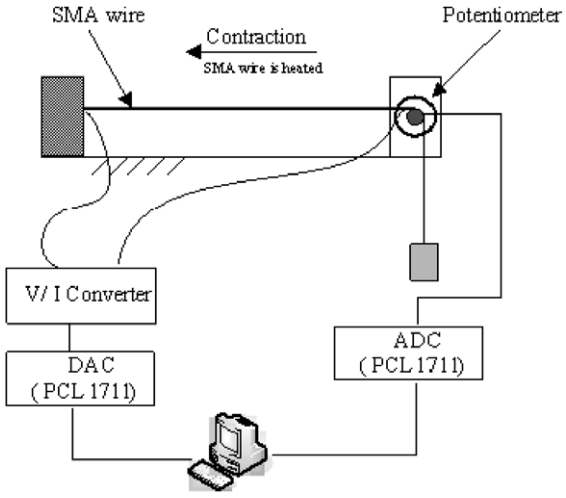

Fig. 7. Experimental apparatus.

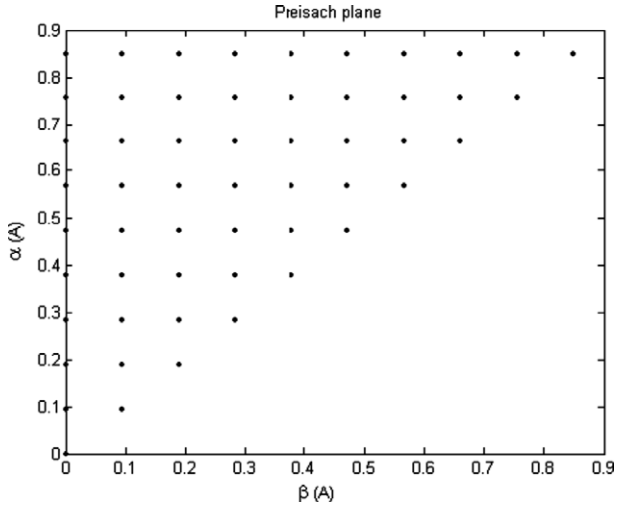

Fig. 8. Number of switching points used in the experiment.

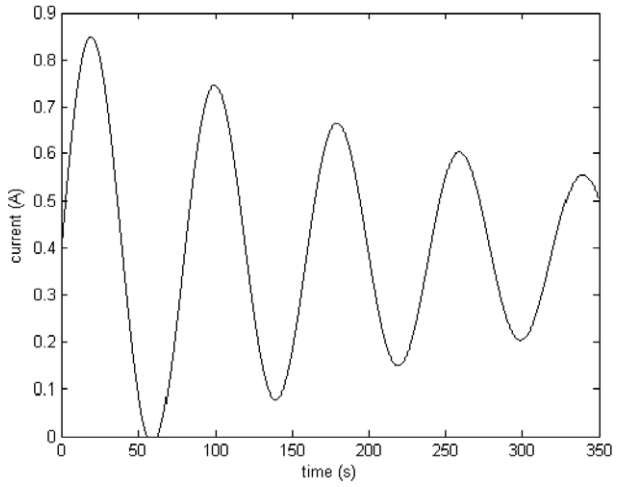

Fig. 9. Input current signal.

used, more accuracy can be obtained by the model. For each switching (α, β) point, the mesh values of the function $F(\alpha, \beta)$ in (4) are computed by measuring the output displacement as the input current is increased to $\alpha(y_\alpha)$ and then decreased to $\beta(y_{\alpha\beta})$.

The input current applied to SMA actuator is a decaying sinusoidal signal, as shown in Fig. 9. During the experiment, the dominant input maxima and minima are determined and updated at each instant of time. The maximum and minimum points are updated by comparing any new dominant extrema with previous extrema. If the value of the input current does not lie at the grid points of the triangle **T** in the Preisach plane, the value of the corresponding $F(\alpha, \beta)$ is determined by four or three point interpolation, which depends on the square or triangle that the input value belongs to.

The output of the hysteresis model, computed from (12) and (14) and the output displacement obtained from the experiment are shown in Fig. 10. In this figure, the experimental result is in good agreement with the of Preisach model prediction.

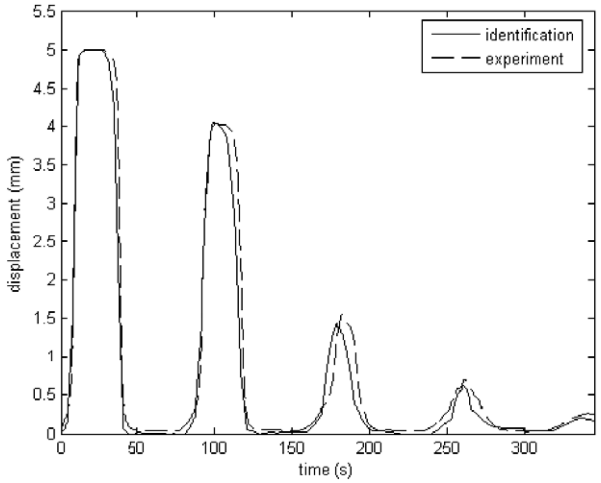

Fig. 10. Comparison of the output displacement through experiment and prediction of the Preisach hysteresis modeling.

The discrepancy between the experiment and model is due to the limited number of switching points available in the corresponding region of the Preisach triangle. This error can be eliminated by increasing the number of points in Preisach plane, as shown in Fig. 8.

3. Simulation of SMA control using PID controller, genetic algorithm and Preisach model

3.1. PID control of SMA actuators

It is observed from the Section 2 that the Preisach model is able to accurately predict the output displacement trajectory from the input current of SMA actuators. In this part, the Preisach model is used in the closed loop PID control scheme to investigate the possibility of the PID algorithm in SMA control in the simulation environment before applying it to real control system. The optimal values of PID parameters are determined by using genetic algorithm in order to obtain the desired output displacement. This control strategy is shown in Fig. 11.

The error between the desired displacement and the output of Preisach model is the input of PID controller. The output of the PID controller is the current applied to the SMA actuator. The optimal values of PID parameters are obtained by using genetic algorithm which is described in the following section. In this work, the Preisach hysteresis model of SMA actuator is programmed as a Simulink block in order to be used in Simulink Toolbox of Matlab.

3.2. Tuning PID parameters using genetic algorithm

Genetic algorithm is well known as a powerful method to solve optimization problems [14]. This algorithm is based on the genetic process of biological organisms.

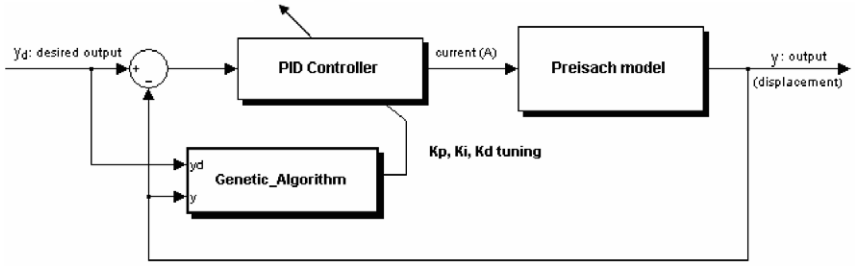

Fig. 11. Turning PID parameters by using genetic algorithm.

Genetic algorithm can deal successfully with a wide range of problem areas, including those which are difficult for other methods to solve.

The principle of genetic algorithm is as follows. A population of individuals is generated; each individual represents a possible solution to a given problem. A new population of possible solutions is produced by selecting the best individuals from the current generation and mating them to produce a new set of individuals. Thus, this new generation contains a higher proportion of the characteristics possessed by the good members of the previous generation. The mutation operation is used to restore lost information and maintain diversity in the population set.

In the current paper, the optimal values of the PID parameters are obtained by using genetic algorithm to minimize the mean squared error between desired output displacement and simulated output from the Preisach model.

The fitness function used in this case is as follows:

$$f(i,K_p,K_i,K_d)=\frac{1}{N}\sum_{i=1}^{N}[y(i)-y_d(i)]^2 \tag{16}$$

where $K_{p\min}\leqslant K_p\leqslant K_{p\max}$, $K_{i\min}\leqslant K_i\leqslant K_{i\max}$, $K_{d\min}\leqslant K_d\leqslant K_{d\max}$ are variation ranges of the PID parameters, i denotes the ith sample time, N is the number of all sample, $y(i)$ and $y_d(i)$ denote the output displacement of the model and the desired output displacement, respectively. Eq. (16) is minimized by using genetic algorithm. The genetic algorithm for this purpose is implemented through the following steps:

Step 1. Encoding and generation of an initial population
First, each variable K_p, K_i, K_d is encoded as an n-bit binary string and these strings are connected to form an individual. Therefore, the length of the individual is $3\times n$. Second, the population size is chosen as M. An initial population of M individuals (chromosomes) is created randomly. $M=100$, $n=16$ are used in this program.

Step 2. Evaluation of the fitness function
After converting the binary individual to the variable representation, these values are used as the parameters of the PID controller. The output displacement of the SMA actuators $y(i)$ is now computed by the Preisach model as shown in Fig. 11. Then the fitness function is calculated by Eq. (16) for each string at every generation.

Step 3. Selection, crossover, and mutation
The individuals are sorted from best to worse according to their fitness evaluations. For each generation, a half of individuals with the highest fitness is selected, and the bottom half of individuals is discarded. Two individuals (strings) swap their binary digits to the right of the crossover points to form the new offsprings. The crossover points are chosen randomly.
Each gene of each individual of the population can mutate independently with given probability by bit–flip operation. This can be used to restore the lost information and maintain the diversity in the population set.

Step 4. Evaluation of new individuals
The new individuals have been created in step 3 are then evaluated by step 2.

Step 5. Termination conditions for the genetic algorithm
The genetic algorithm terminates if one of the two criteria is fulfilled: the given number of generations is reached or the value of the fitness function does not change any more within a certain tolerance. If the best individual meets the termination

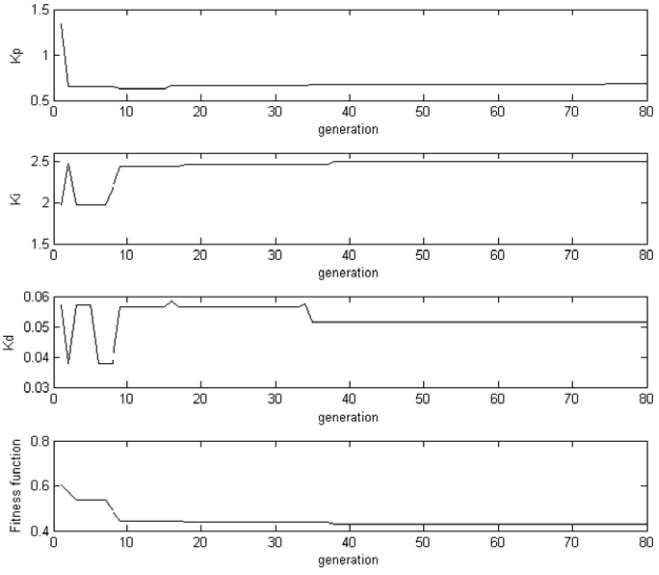

Fig. 12. Results of the PID parameters and fitness function obtained by genetic algorithm.

condition, the genetic algorithm is ended and the best estimation of each parameter is recorded, if not repeat steps 3–5.

With step reference input, the result of the PID parameters obtained from the genetic algorithm is as follows: $K_p = 0.6868, K_i = 2.4966$, $K_d = 0.0516$. The changes of PID parameters and the fitness function are shown in Fig. 12.

3.3. Simulation results

The optimal parameters obtained by the genetic algorithm were used in the PID controllers and the effect of this controller was simulated on the Preisach hysteresis model of the SMA actuators.

The system response respect to step reference input is shown in Fig. 18. The reference signal is the dotted line and the simulated output is the dashed line. From this result, it can be observed that the PID algorithm with the appropriate parameters can be applied to the position control of SMA actuators in the simulation.

4. Application of self tuning fuzzy PID controller to SMA real time control system

Although the simulation results show the effectiveness of the PID controller with parameters obtained by genetic algorithm in SMA control, the performance of this controller is not good when it is applied to the real system. The self tuning fuzzy PID controller is applied to improve the control performance [15–17]. In this work, the PID parameters obtained from the simulation are used as the initial values for tuning these parameters.

The structure of the self tuning fuzzy PID controller is shown in Fig. 13. The controller has the form of PID structure, but the PID parameters are tuned by the fuzzy inference, which provides a nonlinear mapping from the error $e(t)$ (the difference between reference and system output), and derivation of error $de(t)$ to the PID parameters K_p, K_i and K_d. These parameters are tuned from the initial values which are obtained from the simulation.

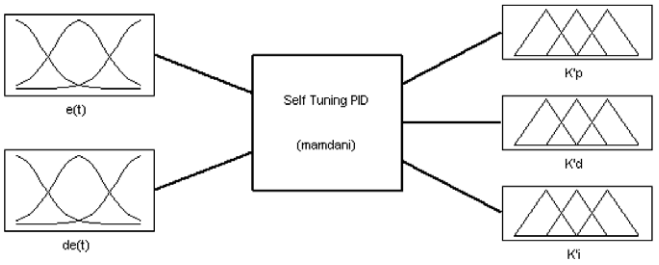

Fig. 14. Structure of the fuzzy inference block.

The stability and robustness analyses of the systems using the fuzzy PID controller have been addressed in several reports [18–22]. In [19], the stability of the closed loop systems composed of a possibly nonlinear plant and the fuzzy PID controller was investigated by Lyapunov function approach. This controller has the similar structure with the controller applied in this work. According to this paper, the Lyapunov function $V(x)$ was firstly established for a closed loop system composed of a plant and a constant parameter PID controller, then the $V(x)$ was also proved to be a Lyapunov function for the closed loop system when the fuzzy PID controller is used. This implied the asymptotic stability of this control structure.

This section presents the implementation of the self tuning fuzzy PID controller for the position control of SMA actuators. The structure of the fuzzy inference block in Fig. 13 is shown in Fig. 14.

4.1. Normalization

From the PID parameters obtained by genetic algorithm, it is convenient to determine the variable ranges for K_p,K_i and K_d as follows: $[K_{p\min}, K_{p\max}]$, $[K_{i\min}, K_{i\max}]$ and $[K_{d\min}, K_{d\max}]$, respectively. The values used in this work are: $K_p \in [0.1, 3]$, $K_i \in [0.5, 5]$ and $K_d \in [0.005, 0.2]$. In order to obtain feasible rule bases with high inference efficiency, the PID parameters must be normalized over the interval $[0, 1]$. Therefore, the real values of the PID parameters are as follows: $K_p = 2.9K'_p + 0.1; K_i = 4.5K'_i + 0.5; K_d = 0.195K'_d + 0.005$, where K'_p, K'_i and K'_d are the normalized values of K_p, K_i and K_d, respectively.

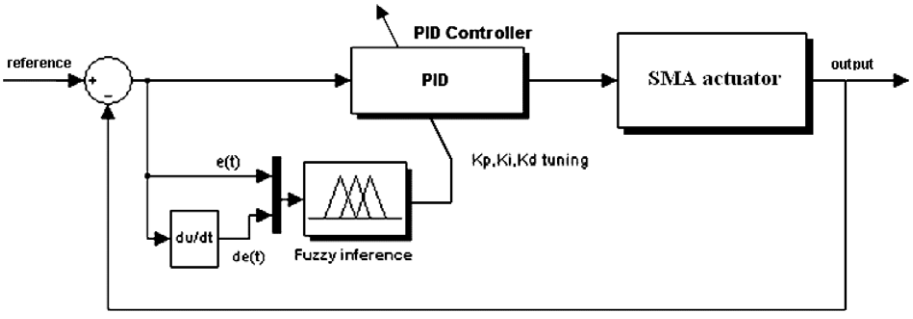

Fig. 13. Structure of the self tuning fuzzy PID controller.

4.2. Fuzzification

In this paper, the linguistic levels assigned to the input variables $e(t)$ and $de(t)$ are as follows: NB: negative big; NM: negative medium; NS: negative small; ZO: zero; PS: positive small; PM: positive medium; PB: positive big.

The membership functions of these fuzzy sets are shown in Fig. 15. The maximum error and the maximum derivation of error ranges are chosen from the specification of SMA actuators.

S, MS, M, B are assigned as the fuzzy sets of K'_p, K'_i and K'_d which are the output variables, and the membership functions of the fuzzy set are shown in Fig. 16.

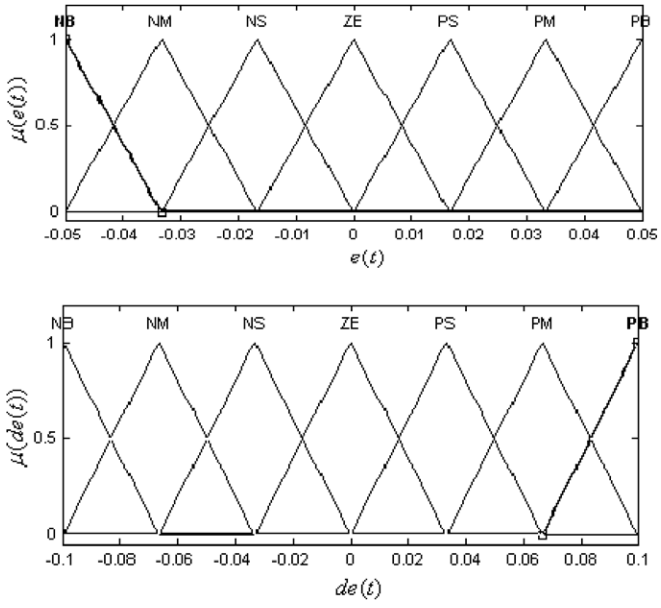

Fig. 15. Membership functions of inputs.

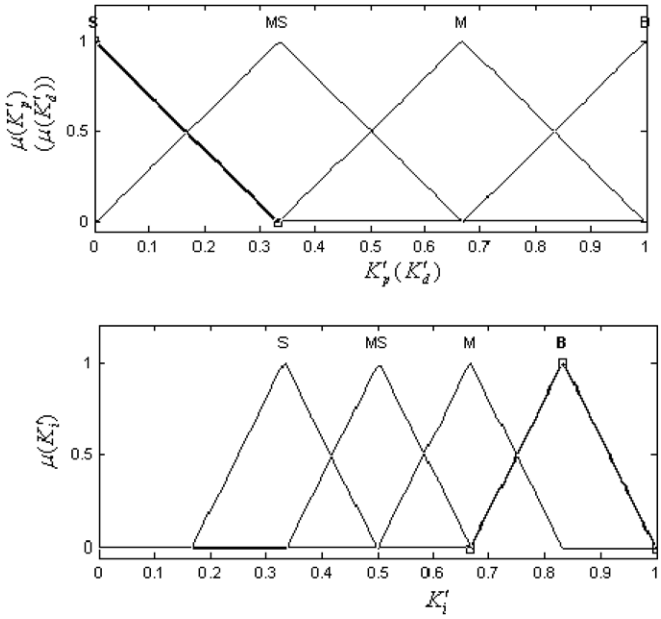

Fig. 16. Membership functions of outputs.

4.3. Fuzzy rule and fuzzy inference

Using the above fuzzy sets of the input and output variables, fuzzy rules are composed as follows:

Rule i: If $e(t)$ is A_i and $de(t)$ is B_i then K'_p is C_i, K'_d is D_i and K'_i is E_i, $i = 1, 2, \ldots, m$, where m is the number of fuzzy rules, A_i, B_i, C_i, D_i, E_i are the ith fuzzy sets of the input and output variables of the fuzzy system. For simplicity, only triangle functions are used as the membership functions, denoted by μ, as shown in Figs. 15 and 16.

Generally, the fuzzy rules are dependent on the plant to be controlled and the type of the controller. These rules are determined from intuition or practical experience. In this paper, rules are designed based on the characteristics of SMA actuators, such as slow response or nonlinear hysteresis effect, and the properties of the PID controller. The rule sets are established and shown in surfaces in Fig. 17.

In this paper, the MAX–MIN fuzzy reasoning method is used to obtain the output from the inference rule and present input. For given a specific input fuzzy set A' in U, the output fuzzy set B' in O for K'_p is computed through the inference engine as follows:

$$\mu'_B(K'_p) = \max_{l=1}^{m}[\sup_{x\in U} \min(\mu_{A'}(x), \mu_{A'_1}(e(t)), \mu_{A'_2}(de(t)), \mu_{B^l}(K'_p))] \tag{17}$$

The output membership functions for K'_d and K'_i are computed similarly.

4.4. Defuzzification

The centroid defuzzification method used in this paper to convert the aggregated fuzzy set to a crisp output value y^* from the fuzzy set B' in $V \subset R$. This work computes the weighted average of the membership function or the center of gravity (COG) of the area bounded by the membership function curves:

$$y^* = \frac{\int_V \mu_{B'}(y) \cdot y \, dy}{\int_V \mu_{B'}(y) \, dy} \tag{18}$$

We compute the crisp value of K'_p, K'_d and K'_i by using the above expression.

4.5. Experimental results

The performance of the proposed control algorithm was investigated for different reference inputs. The sampling time was set to be 0.01 s in all experiments. Fig. 18 shows the performance of the control system with respect to step reference input. From this figure, it can be observed that the self tuning fuzzy PID controller achieves better tracking response than the conventional PID controller without fuzzy tuning.

Figs. 19 and 20 depict the performance of control system respect to sine reference input with two different frequencies. Since the SMA actuator is a slow response system,

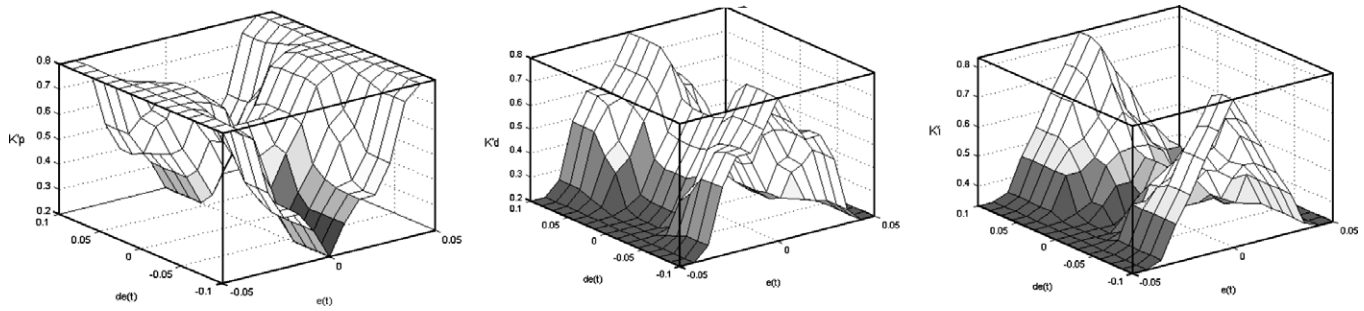

Fig. 17. Fuzzy control rules.

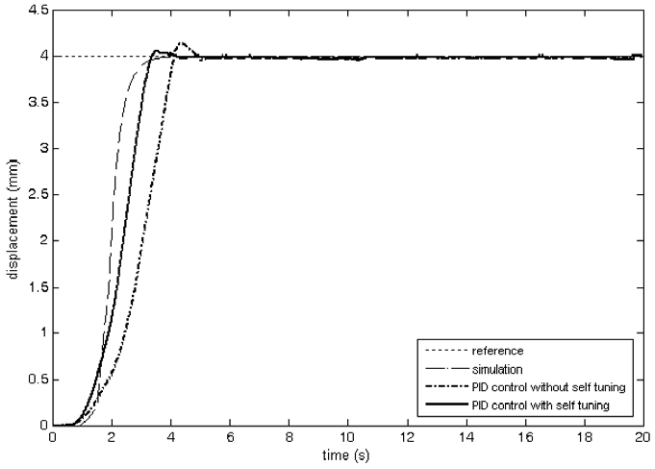

Fig. 18. Step response.

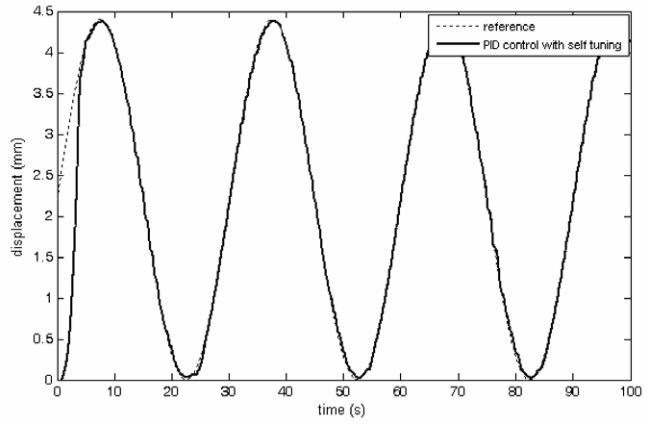

Fig. 20. System response with respect to sine reference input ($f = 0.0333$ Hz).

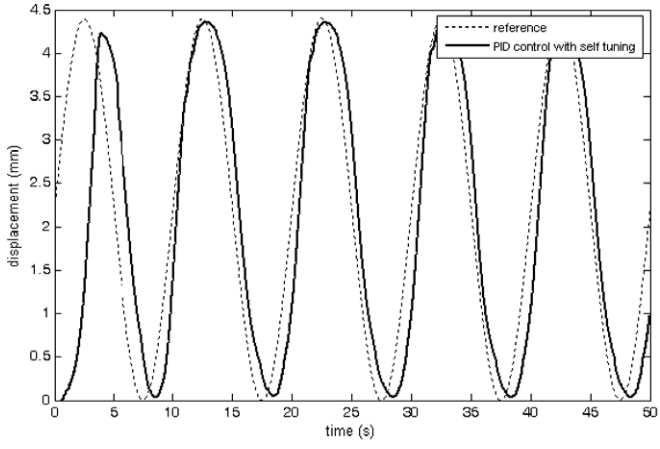

Fig. 19. System response with respect to sine reference input ($f = 0.1$ Hz).

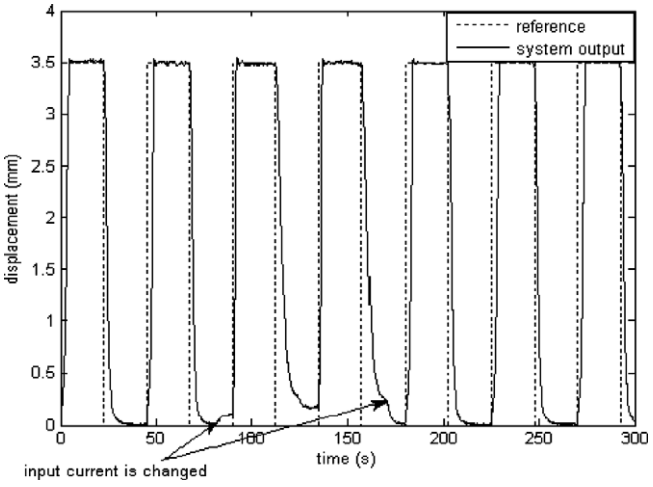

Fig. 21. Effect of the change of input current.

the control performance is better in the low frequency tracking.

The effect of a small variation of input current was also investigated and is shown in Fig. 21. The output displacement keeps good tracking adaptively with the desired trajectory even there is a little change in the input current.

The hysteresis curve between input and output relation of a system including the SMA actuator and controller before (open loop control) and after applying the control algorithm (closed loop control) is shown in Figs. 22 and 23, respectively. The hysteresis curve in Fig. 23 is obtained from the second cycle of the system response with respect to the sine reference signal shown in Fig. 20

Fig. 23 shows nearly the linear relationship between the desired displacement (input) and the system output. There-

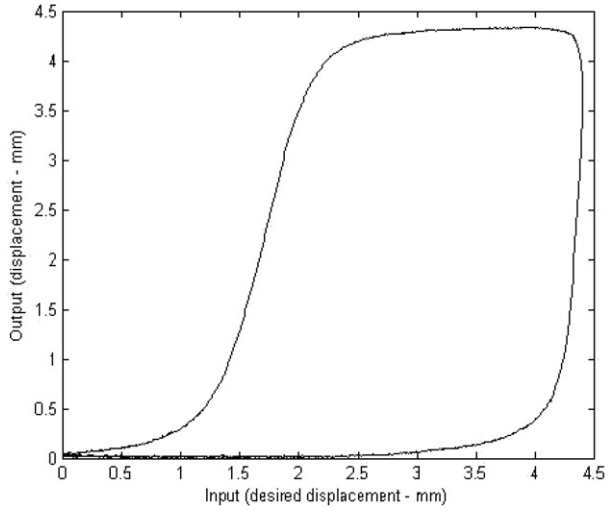

Fig. 22. Hysteresis curve obtained from the experiment before applying control algorithm (open loop control).

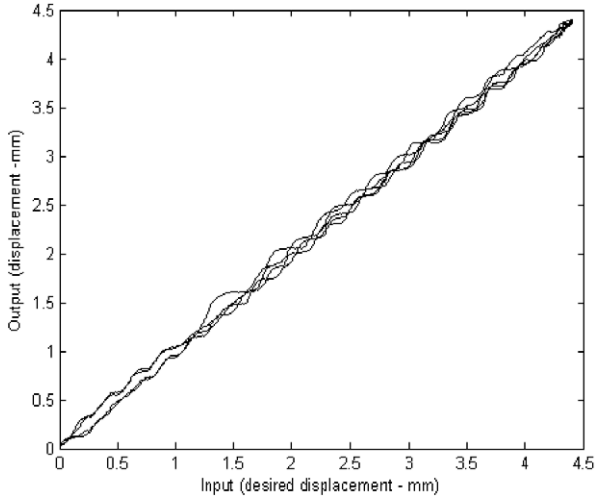

Fig. 23. Hysteresis curve obtained from the experiment after applying control algorithm (closed loop control).

fore, the self tuning fuzzy PID algorithm can be used to reduce hysteresis effect and improve the performance of the position control of SMA actuator in experiment.

5. Conclusion

In this paper, the control problem for SMA actuator was investigated both in simulation and experiment. The numerical Preisach model for the hysteresis in SMA that is based on geometrical implementation has been presented. The experimental evaluation shows that the model is suitable in predicting the hysteresis phenomenon of SMA actuators.

Even though the PID controller with parameters obtained from genetic algorithm demonstrates the effectiveness in the simulation, the control performance was not good in the real control system. The adaptive fuzzy PID controller was developed and successfully applied to the real time position control of SMA actuators. The experimental evaluation showed that the self tuning fuzzy PID controller could adaptively achieve good tracking with respect to different references, a little change of the input current. Therefore, the proposed controller can be used to improve the control performance and reduce the hysteresis effect of SMA actuators.

Acknowledgement

This work was partly supported by the University of Ulsan.

References

[1] Sreekumar M, Singaperumal M, Nagarajan T, Zoppi M, Molfino R. A compliant miniature parallel manipulator with Shape Memory Alloy actuators. In: IEEE international conference on industrial technology, 2006. p. 848–53.
[2] Kode VRC, Çavuşoğlu MC. Design and characterization of a novel hybrid actuator using Shape Memory Alloy and DC micro motor for minimally invasive surgery applications. IEEE/ASME Trans Mech 2007;2(4):455–64.
[3] Smith RC, Massad JE. A unified methodology for modeling hysteresis in ferroelectric, ferromagnetic and ferroelastic materials. In: Proceedings of ASME design engineering technical conference, vol. 6(B), 2001. p. 1389–98.
[4] Mittal Samir, Menq Chia-Hsiang. Hysteresis compensation in electromagnetic actuators through Preisach model inversion. IEEE/ASME Trans Mech 2000;5(4):394–409.
[5] Tan X, Baras JS. Modeling and control of a magnetostrictive actuators. Automatica 2002;40:1469–80.
[6] Hughes D, Wen JT. Preisach modeling of piezoceramic and shape memory alloys hysteresis. Smart Mater Struct 1997;3:287–300.
[7] Viswamurthy SR, Ganguli R. Modeling and compensation of piezoceramic actuator hysteresis for helicopter vibration control. Sensor Actuat A: Phys 2007;135(2):801–10.
[8] Ahn KK, Nguyen BK. Improvement of the performance of hysteresis compensation in SMA actuators by using inverse Preisach model in closed – loop control system. Mech Sci Technol 2006;20(5):634–42.
[9] Ahn KK, Nguyen BK. Internal model control for shape memory alloy actuators using fuzzy based Preisach model. Sensor Actuat A: Phys 2007;136(2):730–41.
[10] Mayergoyz ID. Mathematical models of hysteresis and their applications. Elsevier Science Inc.; 2003.
[11] Basso V, Carlo PS, Martino LB. Thermodynamic aspects of first-order phase transformations with hysteresis in magnetic materials. Magn Magn Mater 2007;316(2):262–8.
[12] Cao S, Wang B, Yan R, Huang W, Yang Q. Optimization of hysteresis parameters for the Jiles–Atherton model using a genetic algorithm. IEEE Trans Appl Supercon 2004;14:1157–60.
[13] Leite JV, Avila SL, Batistela NJ, Carpes WP, Sadowski Jr N, Kuo-Peng P, et al. Real coded genetic algorithm for Jiles–Atherton model parameters identification. IEEE Trans Magn 2004;40:888–91.
[14] Mitsukura Y, Yamamoto T, Kaneda M. Genetic tuning algorithm of PID parameters. In: Proceedings of IEEE international conference on systems, man and cybernetics, vol. 1, 1997. p. 923–8.
[15] Pei J, Zhao LM, Wang DJ, Chu L. Fuzzy PID control of traction system for vehicles. In: International conference on machine learning and cybernetics, vol. 2, 2005. p. 773–7.
[16] Zhang JS, Yu DW, Qi SQ. Structural research of fuzzy PID controllers. In: International conference on control and automation ICCA, vol. 2, 2005. p. 1248–53.

[17] Ahn KK, Nguyen BK. Position control of shape memory alloy actuators using self tuning fuzzy PID controller. Int J Control Automat Syst 2006;4(6):756–62.
[18] Wang P, Kwok P. Analysis and synthesis of an intelligent control system based on fuzzy logic and the PID principle. Intell Syst Eng 1992;1(2):157–71.
[19] Birdwell JD, Wang Y. Lyapunov stability analysis of systems using the fuzzy-PID controller. In: American control conference, vol. 1, 1994. p. 966–70.
[20] Sio KC, Lee CK. Stability of fuzzy PID controllers. IEEE Trans Syst, Man Cybern, Part A 1998;28(4):490–5.
[21] Carvajal J, Chen G, Ogmen H. Fuzzy PID controller: design, performance evaluation, and stability analysis. Inform Sci 2000; 123(3–4):249–70.
[22] Chang WD, Hwang RC, Hsieh JG. A self-tuning PID control for a class of nonlinear systems based on the Lyapunov approach. J Process Control 2002;12(2):233–42.